Available online at www.sciencedirect.com
SCIENCE DIRECT®
Physica C 390 (2003) 363–373
PHYSICA C
www.elsevier.com/locate/physc

Magnetic hysteresis of the magnetoresistance and the critical current density in polycrystalline $YBa_2Cu_3O_{7-\delta}$–Ag superconductors

P. Muné [a,b], F.C. Fonseca [c], R. Muccillo [c], R.F. Jardim [a,*]

[a] Instituto de Física, Universidade de São Paulo, CP 66318, 05315-970 São Paulo, Brazil
[b] Departamento de Física Aplicada, Universidad de Oriente, Las Americas, P.O. Box 90500, Santiago de Cuba, Cuba
[c] Instituto de Pesquisas Energéticas e Nucleares, CP 11049, 05422-970 São Paulo, SP, Brazil

Received 26 March 2002; received in revised form 3 February 2003; accepted 12 February 2003

Abstract

A systematic study of the magnetic hysteresis in transport properties of polycrystalline $YBa_2Cu_3O_{7-\delta}$–Ag compounds has been made based on two kinds of measurements at 77 K and under applied magnetic fields up to 30 mT: critical current density $J_c(B_a)$ and magnetoresistance $R(B_a)$. The $R(B_a)$ curves show a minimum in their decreasing branch occurring at $B = B_{min}$ which was found to be both the excitation current I_{ex} and the maximum applied magnetic field B_{am} dependent. In addition, for a certain value of $B_{am} > 5$ mT, we have observed that B_{min} increases with increasing I_{ex} and reaches a saturation value. The $J_c(B_a)$ curves show a maximum in decreasing applied magnetic fields occurring at $B = B_{max}$. We have also found that B_{max} increases with increasing B_{am} and reaches a saturation value. The minimum in the $R(B_a)$ and the maximum in $J_c(B_a)$ curves were found to be related to the trapped flux within the grains. All the experimental results are discussed within the context of the flux dynamics and transport mechanisms in these high-T_c materials.

PACS: 74.50.+r; 74.60.Jg; 74.60.Ge; 74.80.Bj
Keywords: Weak links; Magnetic hysteresis; Intergranular critical current; Trapped flux

1. Introduction

The transport critical current density, J_c, of polycrystalline high-T_c superconductors has been found strongly hysteretic in low applied magnetic fields, $B_a < 50$ mT. Peterson and Ekin [1] and later Evetts and Glowacki [2] showed the theoretical basis for its explanation. Based on these arguments some authors have developed the intragranular flux-trapping model to calculate $J_c(B_a)$ and fit the experimental data in both $YBa_2Cu_3O_{7-\delta}$ and BSCCO ceramics [3–5]. Good agreement between the experimental data and the theory has been found, but many parameters are involved in the fitting, which limits its credibility. It should be

* Corresponding author. Tel.: +55-11-3091-6896; fax: +55-11-3091-6984.
E-mail address: rjardim@if.usp.br (R.F. Jardim).

0921-4534/03/$ - see front matter © 2003 Elsevier Science B.V. All rights reserved.
doi:10.1016/S0921-4534(03)00802-5

noted, however, that the models developed in Refs. [3–5] have disregarded the magnetization of the intergranular medium. Moreover, it has been assumed that the superconducting grains are embedded in a non-superconducting host, without any intergranular shielding effect. On the other hand, Mahel' and Pivarc [6] have used the two-level magnetic system model [7,8] to explain the magnetic hysteresis of high-temperature cuprates under low magnetic fields in transport and magnetic measurements at different temperatures.

Another interesting aspect regarding the hysteresis in transport properties of high-T_c compounds was given by Chen and Qian [9]. These authors early reported the irreversible behavior of the critical current density $J_c(B_a)$ and the magnetoresistance $R(B_a)$ of $YBa_2Cu_3O_{7-\delta}$ at 77 K under low magnetic field $B_a < 50$ mT. Magnetic hysteresis was found in both types of measurements and attributed to the trapped flux in the loops comprised by superconducting grains and weak links in between. It should be mentioned that hysteresis has been also observed in magnetoresistance measurements under high applied magnetic fields $B_a < 3$ T at different temperatures. These experimental results have been explained by taking into account only the intragranular trapped flux in the samples [10,11].

More recently, Sandim and Jardim [12] have studied the irreversible behavior of the magnetoresistance in $Sm_{1.82}Ce_{0.18}CuO_{4-y}$ compounds at 4.2 K. The appearance of a well defined hysteresis in $R(B_a)$ curves was explained by considering only the intergranular trapped flux in the samples. In their analysis, the intragranular trapped flux was disregarded due to the high value of the first critical field of the grains, H_{c1g}, in these compounds at the measured temperature, as compared to the maximum value of the magnetic field applied to the samples.

In this paper we focus on the magnetic hysteresis of transport measurements of polycrystalline $YBa_2Cu_3O_{7-\delta}$–Ag samples based on two kinds of measurements: critical current density $J_c(B_a)$ and magnetoresistance $R(B_a)$ under low magnetic fields $B_a < 30$ mT at a fixed temperature 77 K. The experimental data strongly suggest the influence of both the intergranular and the intragranular trapped flux in transport properties of these polycrystalline samples. The $J_c(B_a)$ and $R(B_a)$ data are analyzed within the framework of both the intragranular flux-trapping model [3–5] and the intra- and intergranular flux-trapping models [6–8]. In addition, effects of the excitation current on the transport properties of these composite superconductors are also discussed.

2. Experimental procedure

Polycrystalline samples of $YBa_2Cu_3O_{7-\delta}$–x wt.% Ag; $x = 3$ and 10; were prepared by using the sol–gel route as described in detail elsewhere [13]. Thin slabs with typical dimensions of $d = 0.8$ mm (thickness), $w = 2$ mm (width) and $l = 10$ mm (length) were used in all experiments. Transport properties measurements were performed using the conventional dc four-probe technique. Magnetic fields up to 30 mT, generated by a water-cooled copper solenoid, were applied perpendicular to the excitation current, which was injected along the major axis of the samples. Critical current and magnetoresistance measurements were performed using excitation current and magnetic field sweeping rates of $\Delta I_{ex}/\Delta t \sim 10$ mA/min and $\Delta B/\Delta t \sim 0.03$ Oe/s, respectively [12]. The magnetic field accuracy in these experiments was about 0.05 mT.

2.1. Magnetic field dependence of the superconducting critical current density $J_c(B_a)$

We have measured $J_c(B_a)$ under three different procedures. In the first one, the superconducting critical current density dependence on applied magnetic field $J_c(B_a)$ was obtained by cooling the sample from room temperature down to 77 K under zero applied magnetic field. Then, the magnetic field was increased from zero to a fixed value B_a and the excitation current, I_{ex}, through the sample was increased. Under these circumstances, we have measured V versus I_{ex} and the $J_c(B_a)$ value was defined as the excitation current in which the voltage across the sample was ~ 1 μV. This procedure was repeated several times for different fixed values of B_a, $0 \leqslant B_a \leqslant 30$ mT. From the values of J_c at different B_a values, we obtained

the $J_c(B_a)$ dependence for increasing applied magnetic field. This curve is referred as *virgin curve*.

The curves obtained in the second procedure were referred here as *returning curves*. In these measurements, the sample was cooled down to 77 K under zero applied magnetic field. Then, the magnetic field was increased and established to a given B_{am} value. After this step, the magnetic field was decreased from B_{am} to a fixed value B_a and the excitation current I_{ex} through the sample was increased automatically to determine the critical current density. The following steps were the same as described above. However, it is worth mentioning that, in this case, the J_c values were obtained under a given applied magnetic field B_a which is fixed, after the sample was subjected to a certain maximum value B_{am}, $B_a < B_{am}$. After the application of B_{am}, the different values of B_a were applied in progressively lower magnitudes.

The last procedure corresponds to the so-called *flux-trapping curve* [14]. The samples were cooled in the same conditions as described above. Then, a certain value of magnetic field B_{am} was applied during ~30 s. After that, the magnetic field was abruptly removed and the critical current was measured as described in the first procedure. Under these conditions, the critical current of the sample was measured as described in the first procedure. As last step the sample was warmed at temperatures higher than its superconducting critical temperature and cooled down to 77 K in zero applied magnetic field before measuring another value of the dependence $J_c(0, B_{am})$. By repeating these steps for different values of B_{am} the flux-trapping curve was obtained.

2.2. Magnetoresistance $R(B_a)$

In all magnetoresistance measurements the samples were first cooled from room temperature to 77 K in zero applied magnetic field and an excitation current ranging from 50 to 750 mA was used. After this step, the magnetic field was increased from zero to a maximum value, B_{am}, and then it was decreased to zero. During the magnetic sweep, a computer controlled all the measuring process and collected the experimental data.

When the B_{am} value was changed to obtain the different $J_c(B_a)$ and $R(B_a)$ data, special care was taken to eliminate the magnetic history of the samples. In all cases, the sample was warmed up to temperatures close to 120 K and cooled down to 77 K before further measurements.

3. Experimental results and discussion

3.1. The $J_c(B_a)$ dependence

It is useful to start this discussion by showing the normalized transport critical current density data, $J_c^n(B_a) = J_c(B_a)/J_c(0)$, as displayed in Fig. 1. This figure shows the experimental data of $J_c^n(B_a)$ for a $YBa_2Cu_3O_{7-\delta}$–3 wt.% Ag slab-like sample as a function of both, the increasing and the decreasing field from different maximum fields B_{am}. The inset displays some of these curves, but the normalized critical current density has been substituted by the absolute values of the critical current. Some relevant features, besides the clear

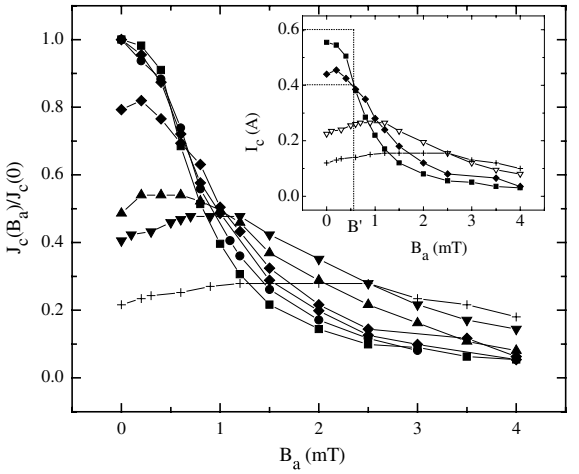

Fig. 1. Normalized critical current density as a function of the applied magnetic field for the sample $YBa_2Cu_3O_{7-\delta}$–3 wt.% Ag: virgin curve (■), returning curve from 4 mT (○), returning curve from 5 mT (◇), returning curve from 6 mT (◆), returning curve from 8 mT (▲), returning curve from 10 mT (▽), returning curve from 26 mT (+). The inset shows some of these curves, but the normalized critical current density has been substituted by the critical current.

hysteresis of $J_c^n(B_a)$ can be extracted from these curves:

(a) The returning curves obtained in fields $B_{am} > 5$ mT show a well defined peak in the $J_c(B_a)/J_c(0)$ dependence. Such a peak occurs at a given magnetic field B_{max}.
(b) A careful inspection of these curves reveals that the peak position of J_c^n at B_{max} shifts to higher values with increasing B_{am}. Furthermore, the peak of J_c^n broadens and decreases its height with increasing B_{am}.
(c) For $B_{am} > 20$ mT, differences between returning curves are negligible.
(d) A small, but appreciable, difference between virgin and returning curves is observed for $1 \leqslant B_a \leqslant 2$ mT, when $B_{am} \leqslant 5$ mT.

Similar results to the ones shown in Fig. 1 have been found by other authors in polycrystalline $YBa_2Cu_3O_{7-\delta}$ samples [3,4].

The *flux-trapping curve* of the same 3% Ag sample is displayed in Fig. 2 which shows the J_c data taken at zero applied magnetic field $J_c^n(0, B_{am})$ as a function of B_{am}. The results indicate that $J_c^n(0, B_{am})$ is essentially constant for $B_{am} < 5$ mT. On the other hand, for $B_{am} > 5$ mT it decreases appreciably and reaches a saturation value at ~20 mT.

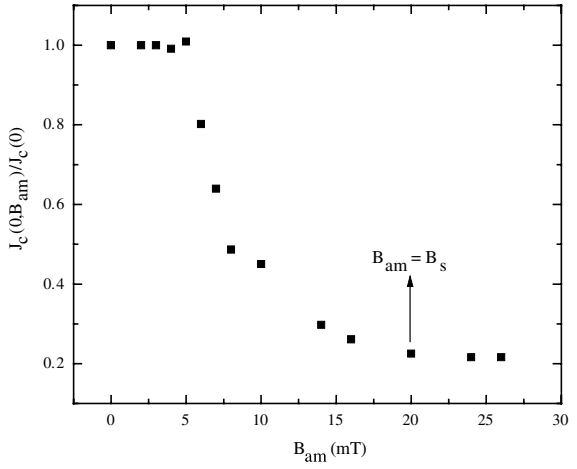

Fig. 2. Normalized critical current density at zero applied magnetic field as a function of the maximum applied magnetic field B_{am} of the sample $YBa_2Cu_3O_{7-\delta}$–3 wt.% Ag.

By combining the results shown in Figs. 1 and 2 one is able to distinguish three different ranges of B_{am} in which the irreversible behavior of the $J_c^n(B_a)$ dependence has different regimes, as described below.

(1) For $B_{am} \leqslant 5$ mT: there are appreciable differences between the virgin and the returning curves for $1 < B_a < 2$ mT. The peak position and height of J_c^n show no appreciable changes.
(2) For $5 < B_{am} \leqslant 20$ mT: the peak position of J_c^n shifts to higher values and decreases its height with increasing B_{am}. Appreciable differences between the virgin and the returning curves can be observed in all the range of B_a. These differences increase when B_{am} increases.
(3) For $20 < B_{am} \leqslant 26$ mT: the shape of the curves seem to be independent of B_{am}. No appreciable differences between the returning curves in this range are observed.

3.2. The $R(B_a)$ dependence

The $R(B_a)$ results are meaningful for the discussion involving the hysteretic behavior of the transport properties in these cuprates. In particular, Fig. 3 shows two $R(B_a)$ curves of the $YBa_2Cu_3O_{7-\delta}$–3 wt.% Ag sample in magnetic fields up to $B_{am} = 8$ and 10 mT, when the sample was subjected to the same excitation current $I_{ex} = 400$ mA. Some interesting features are observed in these curves. First, a clear hysteresis is found when the magnetic field is increased and decreased from a maximum value B_{am}. Secondly, the magnitude of $R(B_a)$ is lower in the decreasing branch for most of the measured range of B_a, but such a behavior changes at low fields $B_a < 1$ mT, and an appreciable increase in the magnitude of $R(B_a)$ is observed. However, the most significant feature of these curves is the occurrence of a minimum in the decreasing branch of $R(B_a)$ at a magnetic field near $B_{min} \approx 0.45$–0.8 mT (see inset of Fig. 3).

We have also observed that the position of this minimum shifts to higher values with increasing B_{am}. It should be noticed that B_{min} observed in the decreasing branch of $R(B_a)$ curves has its coun-

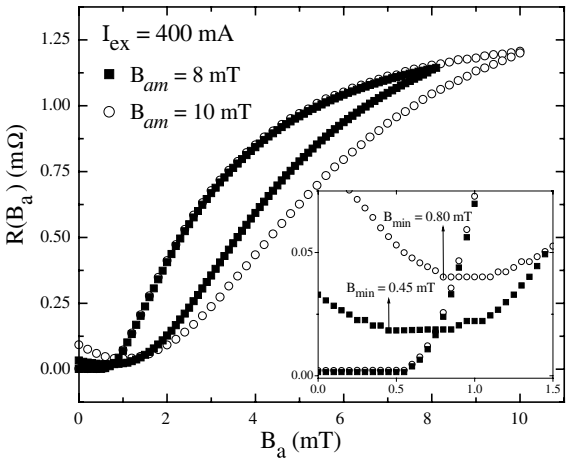

Fig. 3. Magnetoresistance curves taken on the polycrystalline sample of $YBa_2Cu_3O_{7-\delta}$–3 wt.% Ag for two different values of the maximum applied magnetic field: $B_{am} = 8$ mT (■) and $B_{am} = 10$ mT (○). The inset shows the curves for $0 < B_a < 1.5$ mT. Arrows indicate increasing and decreasing applied magnetic field.

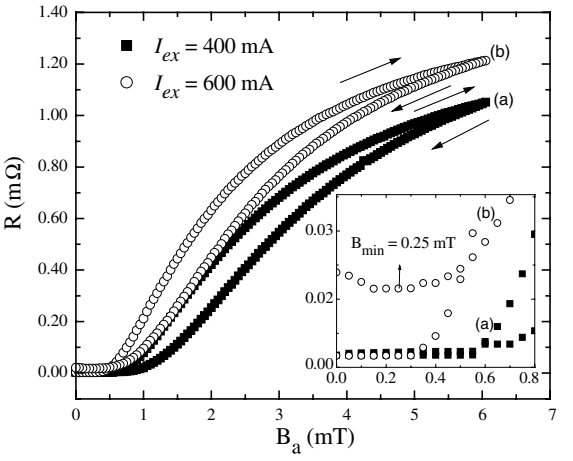

Fig. 4. Magnetoresistance curves taken on the sample $YBa_2Cu_3O_{7-\delta}$–3 wt.% Ag for two different values of excitation current: $I_{ex} = 400$ mA (■) and $I_{ex} = 600$ mA (○). Arrows denote increasing and decreasing applied magnetic field. The inset shows an expanded view of the low applied magnetic field behavior.

terpart in the $J_c(B_a)$ data. In fact, a careful observation of the curves shown in Figs. 1 and 3 reveals that $B_{max} \approx B_{min}$ when both $J_c^n(B_a)$ and $R(B_a)$ curves are taken at the same value B_{am}.

Additional information regarding the hysteresis in $R(B_a)$ curves can be obtained when the sample is subjected to different excitation currents. In order to discuss this point, Fig. 4 displays the $R(B_a)$ curves obtained for two different excitation currents, i.e., $I_{ex} = 400$ mA (a) and 600 mA (b). In both measurements B_{am} was fixed at 6 mT. The most pronounced difference between these two curves is the absence of a minimum in the decreasing branch of the curve taken at the lower excitation current, i.e., $I_{ex} = 400$ mA (curve (a)). Here, the excitation current is lower than the critical current of the sample for magnetic fields lower than B', as shown by a dotted line in the inset of Fig. 1. On the other hand, the decreasing branch of the curve (b) displays a minimum at $B_{min} \approx 0.25$ mT. Also, this value of B_{min} corresponds to the one where J_c peaks in the $J_c(B_a)$ curve for $B_{am} = 6$ mT (see Fig. 1). It is worth mentioning that for decreasing fields, the difference $I_{ex} - I_c$ decreases for $B_{max} < B_a < B_{am}$, but it increases when $0 < B_a < B_{max}$ (see Fig. 1). A similar analysis would be applied to determine when a given value of the excitation current causes a minimum in the decreasing branch of the $R(B_a)$ curve for a certain value of applied magnetic field B_{am}.

Figs. 5 and 6 display the hysteretic behavior of $R(B_a)$ curves taken in magnetic fields up to $B_{am} = 4$ and 10 mT, respectively. Similarly to the case of the $J_c^n(B_a)$ dependence, we have found that the difference between increasing and decreasing branches increases with increasing B_{am}. Another relevant result for the following discussion was obtained from $R(B_a)$ curves measured at a fixed $B_{am} = 10$ mT and for different excitation currents. These results are shown in Fig. 6 for $I_{ex} = 250$ and 650 mA. The data reveal that B_{min} increases with I_{ex} and reaches a saturation value for $I_{ex} = I_s \approx 550$ mA, as shown in the inset of Fig. 6.

From several $R(B_a)$ curves measured under 10 mT and subjected to different excitation currents, we have obtained not only the B_{min} values but also the minimum voltage across the sample at B_{min}. These results are shown in Fig. 7, which displays V_{min} as a function of excitation current for the sample $YBa_2Cu_3O_{7-\delta}$–3 wt.% Ag. The results clearly show that no minimum voltage is observed

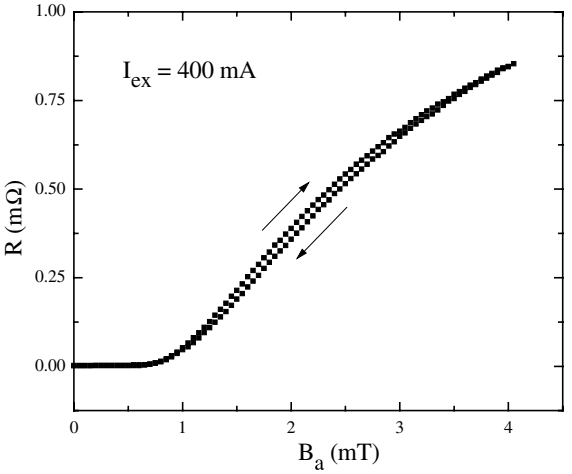

Fig. 5. Magnetoresistance curve taken on the sample $YBa_2Cu_3O_{7-\delta}$–3 wt.% Ag for $B_{am} = 4$ mT and $I_{ex} = 400$ mA. Arrows indicate increasing and decreasing applied magnetic field.

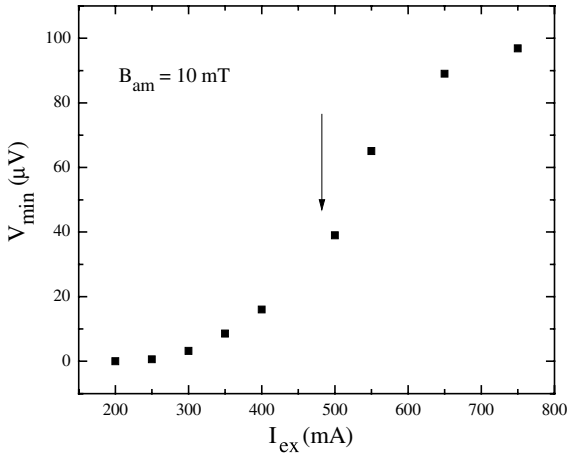

Fig. 7. Excitation current–voltage characteristics for the sample $YBa_2Cu_3O_{7-\delta}$–3 wt.% Ag. This curve was built by plotting the minimum voltage of the decreasing branch of $R(B_a)$ curves measured at different excitation currents versus the excitation current.

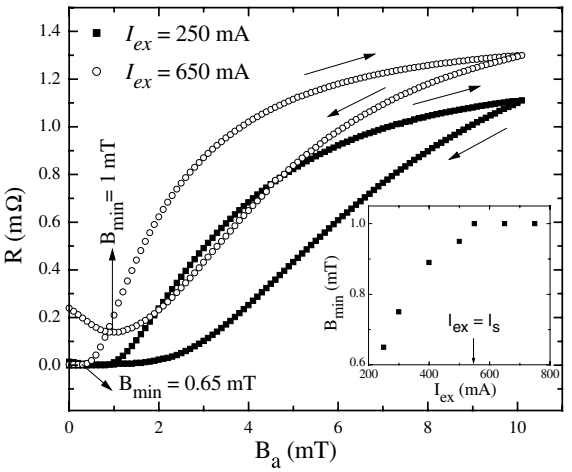

Fig. 6. Magnetoresistance curves taken on $YBa_2Cu_3O_{7-\delta}$–3 wt.% Ag sample for two different values of excitation current: $I_{ex} = 250$ mA (■) and $I_{ex} = 650$ mA (○). The inset shows the B_{min} as a function of the excitation current. Arrows indicate increasing and decreasing applied magnetic fields.

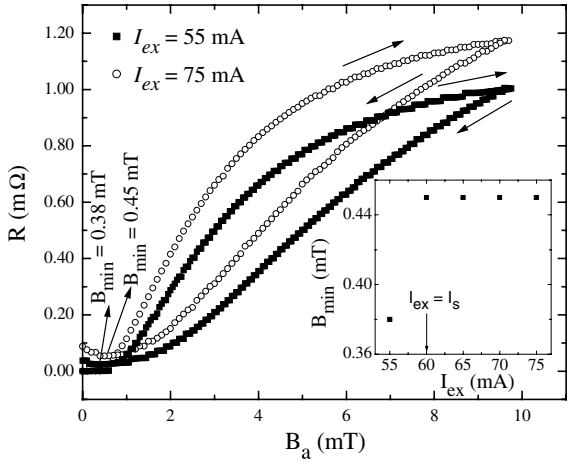

Fig. 8. Magnetoresistance $R(B_a)$ curves taken on the sample $YBa_2Cu_3O_{7-\delta}$–10 wt.% Ag for two different values of excitation current: $I_{ex} = 55$ mA (■) and $I_{ex} = 75$ mA (○). The inset displays B_{min} as a function of the excitation current. Arrows indicate increasing and decreasing applied magnetic field.

for excitation currents below ~300 mA. However, increasing I_{ex} results in a smooth increase of the minimum voltage up to $I_{ex} \sim 500$ mA and such an increase is faster for $I_{ex} > 500$ mA.

Similar measurements were performed in samples with different Ag content, i.e., $YBa_2Cu_3O_{7-\delta}$–10 wt.% Ag. For these measurements, slab-like samples were cut with the same dimensions as the sample with 3 wt.% Ag. The relevant results for the following discussion are shown in Fig. 8. This

figure displays $R(B_a)$ curves taken up to $B_{am} = 10$ mT when the sample was subjected to different excitation currents: 55 and 75 mA. The typical excitation current used in these experiments was one order of magnitude lower than those of the sample $YBa_2Cu_3O_{7-\delta}$–3 wt.% Ag. Generally speaking, the results are similar to the ones shown in Fig. 6: the position of the minimum B_{min} in the decreasing branch of the curve shifts to higher values of B_a with increasing I_{ex}. However, the shift of B_{min} with increasing I_{ex} is appreciably lower than the ones found in the sample with 3 wt.% Ag.

3.3. Discussion

3.3.1. The intragranular flux-trapping model

The essence of the *intragranular flux-trapping model* is to consider weak links or even Josephson junctions embedded in an effective magnetic field B_i resulting from the competition between the external field and the field associated with the magnetization of the grains. The grains are supposed to follow Bean's critical state model [15], which has been modified to take into account the first critical field, H_{c1g} [4]. By considering this, B_i can be written as follows:

$$B_i = B_a - \mu_0 G M_g \tag{1}$$

where μ_0 is the magnetic permeability of vacuum, G is the geometric factor of the grains in the array and M_g is the intragranular magnetization.

Following this model, the hysteretic behavior in transport measurements has its origin closely related to the hysteretic behavior of the intragranular magnetization, M_g. Therefore, the shape of both $J_c^n(B_a)$ and $J_c^n(0, B_{am})$ dependence have been successfully reproduced using this model, as discussed elsewhere [3,4,14]. We also argue that the theoretical basis used in these references can be applied to our results since both experimental results are qualitatively very similar.

As the shift and the decrease of the maximum seem to be the most relevant features of the hysteretic behavior of the $J_c^n(B_a)$ dependence, we reproduce here the main ideas of the usual explanation of this phenomenon by using the *intragranular flux-trapping model* [3,4]. The $J_c^n(B_a)$ dependence attains its maximum value when the field B_i between grains is zero and thus from Eq. (1) one obtains for the field B_{max} in which J_c^n peaks:

$$B_{max} = \mu_0 G M_g(B_i = 0, B_{am}) \tag{2}$$

where $M_g(B_i = 0, B_{am})$ increases for $B_{im} > \mu_0 H_{c1g}$ and it saturates for $B_{im} > \mu_0(H_{c1g} + 2H^*)$. Here, B_{im} is the intergranular field when the applied magnetic field is B_{am} and H^* is the full penetration field of the grains according to the Bean's model. Based on these ideas and the results for the $YBa_2Cu_3O_{7-\delta}$–3 wt.% Ag sample shown in Figs. 1 and 2, one obtains $\mu_0 H_{c1g} \approx 5$ mT and $\mu_0 H^* \approx 7.5$ mT as a first approximation [14]. Furthermore, the broadening of the peak and its decrease in magnitude have their origins in the statistical distribution of geometric factors G and other inter- and intragranular properties.

Similar explanations can be used for the change of B_{min} in the $R(B_a)$ dependence when B_{am} is increased. However, $B_i = 0$ corresponds to a maximum in $J_c^n(B_a)$ curves but with a minimum in $R(B_a)$ dependence. This occurs because the voltage across the sample is expected to decrease with decreasing B_i within the framework of dissipation models in a granular superconductor [1,16]. This last statement is confirmed by our experimental results where B_{max} in $J_c(B_a)$ curves and B_{min} in $R(B_a)$ data are very similar for the same value of B_{am}.

We intend to explain now, at least qualitatively, changes observed in B_{min} with increasing I_{ex} in the $R(B_a)$ curves, as shown in Figs. 3–6, by using the intragranular flux-trapping model [3,4]. Following Eq. (2), changes observed in either B_{max} ($J_c^n(B_a)$ curves) or B_{min} ($R(B_a)$ curves) only occur if M_g ($B_i = 0, B_{am}$) or G are altered. Increasing the excitation current through the sample may affect M_g by two main reasons:

(1) The relaxation of the granular magnetization M_g due to intragranular flux creep [17].
(2) The suppression or weakening of the superconductivity inside some grains that have very low critical current, taking into account the wide distribution of the physical properties in these granular materials.

In these two assumptions both M_g and B_{min} are expected to decrease with increasing I_{ex}. However, our experimental results show the opposite, at least for the B_{min} behavior. In fact, increasing I_{ex} results in an *increase* of B_{min} and its saturation for higher I_{ex} (see Figs. 6 and 8). This indicates that the arguments above mentioned seem to be inappropriate in explaining the behavior observed in these measurements. Moreover, if one estimates the mean value of the intragranular current density J_{cg} for the sample $YBa_2Cu_3O_{7-\delta}$–3 wt.% Ag by using the flux-trapping curve [3,4,14] (see Fig. 2) and assuming the mean size of the grains $D = 15$ μm [13], one obtains $J_{cg} = (H_s - H_{c1g})/D = 8 \times 10^4$ A/cm^2. Such a value of J_{cg} is very high as compared to the values of the excitation current density used in our measurements, typically $J_{ex} \cong 50$ A/cm^2. This strongly suggests that the excitation currents used in our measurements do not affect appreciably the intragranular magnetization of the sample.

The other parameter to take into account in this discussion is G. It can be mainly affected by the suppression of superconductivity in some grains when I_{ex} is increased. As we have used low magnitude of both excitation current and magnetic field values in these experiments, this would result in a condition similar to the one described in (2), which has been analyzed already.

Based on the above considerations, we argue that the shift of B_{min} with increasing excitation current I_{ex} could not be explained within the framework of the intragranular flux-trapping model.

3.3.2. The intra- and intergranular flux-trapping model

In this model, the ceramic is regarded as a two-level magnetic system, consisting of superconducting grains and a weak-link network forming a quasi-continuous superconducting intergranular medium both treated as type II superconductors [6–8]. In this case three components have to be taken into account: (1) the applied magnetic field, B_a; (2) the contribution of the intragranular magnetization, M_g and (3) the contribution of the intergranular magnetization, M_i. Within this context Mahel' and Pivarc have obtained the following expression for the intergranular magnetic field [6]:

$$B_i = B_a + \mu_0(M_i(1 - N_s) - (CN_s + G)M_g) \tag{3}$$

where N_s is the geometrical factor of the sample and C is a factor, which depends on the volume fraction occupied by the grains in the sample. Let us suppose that $N_s = 0$ to simplify our analysis. Then, Eq. (3) can be written as follows:

$$B_i = B_a + \mu_0(M_i - GM_g) \tag{4}$$

The most relevant point regarding Eq. (3) relies on the fact that M_i and M_g have opposite contributions to the intergranular magnetic field. Within this context, and in the limit of low applied magnetic fields, two points are of interest. First, the critical state of the grains can be described by Bean's model because $J_{cg} =$ constant. Secondly, the case is quite different at sample level because the intergranular current density decreases rapidly with increasing B_i. Under this circumstance, the intergranular magnetization is believed to be better described by Kim's model [18], although Bean's model could be used as a first approximation. In a similar way to the last section, the $J_c^n(B_a)$ dependence is maximal or $R(B_a)$ is minimal when $B_i = 0$. Indeed, by taking $B_i = 0$ Eq. (4) is described by

$$B_{max} = \mu_0(GM_g(B_i = 0, B_{am}) - M_i(B_i = 0, B_{am})) \tag{5}$$

We would like to point out two aspects regarding the above equation (5):

(1) Two different kinds of magnetization determine the position of the peak in $J_c^n(B_a)$ or the minimum in $R(B_a)$.
(2) Considering M_i at the level of the sample (as in Eq. (5)) is relevant only for very low intergranular magnetic fields, or more appropriately close to the minimum or the peak in $R(B_a)$ or $J_c^n(B_a)$, respectively. This is because increasing B_i results in a decrease of the area of the current loops. Such a decrease is expected to vary from the sample dimension to the grain dimension [12,19]. Under this condition Eq. (5) is not expected to be valid.

Following the point (1) above mentioned, we have noticed that M_i and M_g are different because the intragranular critical current density is very

high as compared to the intergranular critical current density. Thus, the intergranular flux creep and flux flow could be observed even when the grains are in the critical state [17]. In addition, $M_i \ll M_g$ by considering the dimensions and the critical current density of the grains and of the sample, respectively. Within this scenario, it is reasonable to assume that the hysteretic behavior of both $J_c^n(B_a)$ and $R(B_a)$ dependence is mainly determined by the hysteretic behavior of the intragranular magnetization. This approximation seems to be valid in the limit of high current densities and high values of B_i since under these circumstances the intergranular critical state is suppressed. In other words, the intra- and intergranular flux-trapping model is reduced to the intragranular flux-trapping model in the limit of high current densities and high intergranular magnetic fields.

After these considerations, we are able to propose an explanation to the observed shift of the B_{min} with increasing I_{ex} in these ceramics. When I_{ex} is increased, M_i first relaxes and decreases essentially due to flux creep [16] and then it becomes zero due to flux flow [7,12,20]. Under this condition, the position of B_{min} is determined by an equation similar to Eq. (2). Then, the results shown in the insets of Figs. 6 and 8 can be interpreted as the transition of the sample from the intergranular flux creep to the intergranular flux flow regime. In our analysis we have also considered that the intragranular magnetization is not affected by the transport current taking into account aspects discussed in the last section. In addition, similar arguments can be applied to explain the results shown in Fig. 7. When the material is in the flux creep regime, the voltage across the sample increases slowly with increasing excitation current. At low excitation current a small number of intergranular fluxons have enough thermal energy to be moved by the Lorentz force from one pinning center to another or even out of the sample. The amount of fluxons is expected to increase with increasing current until the Lorentz force is greater than the pinning force. For this excitation current, the system undergoes a transition from flux creep to flux flow regime. Such a transition is mirrored in the $R(B_a)$ data, as shown in the inset of Fig. 6. There, the saturation current $I_s \approx 550$ mA corresponds to the value of the excitation current in which the transition from flux creep to flux flow regime occurs. In addition, it is expected that the voltage across the sample increases linearly with increasing excitation current. A careful inspection of Fig. 7 reveals that for $I_{ex} > 500$, in spite of the small number of experimental data points, the V_{min} versus I_{ex} curve follows approximately a linear trend, which indicates the flux flow regime. This means that the values of I_{ex} at the boundary of the flux creep to flux flow regime are similar even though they have been determined using different kinds of measurements.

Eq. (5) and the second aspect related to it can lead us to other conclusions. The intergranular magnetization at the level of the sample cannot produce a minimum in the $R(B_a)$ curves at positive values of applied magnetic field. This occurs because its contribution has the same sign of the applied magnetic field. In fact, the magnetization of type II superconductors in the mixed state, which is opposite to the applied magnetic field when it is increased, eventually reverses its sign for decreasing applied magnetic fields [15,18]. Thus, M_i, M_g, and B_a are expected to have the same sign, but the intragrain contribution in the intergranular region is opposite to the other two components [6]. Then, the minimum in the $R(B_a)$ curve (or the maximum in $J_c^n(B_a)$ ones) seems to be related to the trapped flux within the grains, or in levels with dimensions lower than the dimensions of the sample, like superconducting clusters for example. This last conclusion is in complete agreement with previous results [3,4].

Far away from the minimum in the $R(B_a)$ curve (or the maximum in $J_c^n(B_a)$ dependence) the areas of the intergranular loops decrease due to the increase of the intergranular field. Then, the presence of these loops could explain the small differences between the increasing and decreasing branch of both the $J_c^n(B_a)$ and $R(B_a)$ dependence when $B_{am} <$ 5 mT (see Figs. 1 and 5). The dynamics of these loops should be to increase their areas with decreasing B_i, reaching the dimension of the sample close to $B_i = 0$ [12,19].

In order to lend credence to our interpretation on the shift of B_{min} with increasing I_{ex}, ΔB_{min}, we

have determined such a shift when I_{ex} is increased from a certain value for which the minimum appears until I_s (see Figs. 6 and 8). Assuming that ΔB_{min} is determined by the relaxation of the intergranular magnetization M_i and using Bean's model one obtains $M_i(B_i = 0, B_{am}) \propto J_{cp}$, where J_{cp} is the critical current density of the sample in the peak position. Then, the ratio between the ΔB_{min} of both samples with different values of J_{cp} should be equal to the relation between their J_{cp} values. Our samples with different wt.% Ag content satisfy the last relation including the error in determining ΔB_{min} as follows:

$$\frac{\Delta B_{min\,1}}{\Delta B_{min\,2}} = \frac{(0.35 \pm 0.05)\ \mathrm{mT}}{(0.07 \pm 0.05)\ \mathrm{mT}} \approx 5.0 \pm 3.5 \quad \text{and} \quad \frac{J_{cp1}}{J_{cp2}} \approx 4.5$$

where the subscripts 1 and 2 correspond to the samples $YBa_2Cu_3O_{7-\delta}$–3 wt.% Ag and $YBa_2Cu_3O_{7-\delta}$–10 wt.% Ag, respectively. Since both samples have similar dimensions, the ratio between their critical current densities can be estimated by the ratio between their critical currents. The critical current of the sample with 3 wt.% Ag in the peak of the returning curve from 10 mT is ~250 mA (see Fig. 1) while that for the sample with 10 wt.% Ag was found to be ~55 mA. The estimated values, including the error arising from the magnetic field, are of the same order of magnitude. However, the mean values differ by less than 10% which represents a good agreement between the model and the experimental data.

4. Conclusions

In summary, we have observed that the magnetic dependence of both the magnetoresistance $R(B_a)$ and the critical current density $J_c(B_a)$ of polycrystalline samples of $YBa_2Cu_3O_{7-\delta}$–x wt.% Ag; $x = 3$ and 10; reveal a strong hysteretic behavior. For a certain value of the maximum applied magnetic field B_{am}, these $R(B_a)$ and $J_c(B_a)$ curves exhibit a minimum and a maximum, respectively. We also found that these minima in $R(B_a)$ and maxima in $J_c(B_a)$ occur at almost the same value of applied magnetic field in their decreasing branches. These critical points shift to higher values of applied magnetic field with increasing B_{am} and then they saturate. We observed that this shift is mainly determined by the hysteretic behavior of the intragranular magnetization in a similar way as have been earlier reported in $J_c(B_a)$ curves for $YBa_2Cu_3O_{7-\delta}$ [3,4]. On the other hand, the shift of the minimum in the $R(B_a)$ curves with increasing excitation current seems to be related to the intergranular magnetization, which evolves from flux creep to flux flow regime with increasing excitation current.

Acknowledgements

The authors have benefited from the technical assistance of Walter Soares de Lima. This work was supported by the Brazilian agency Fundação de Amparo à Pesquisa do Estado de São Paulo (FAPESP) under grant no. 99/10798-0. Two of us PM and FCF are FAPESP fellows under grant nos. 99/05678-6 and 01/04231-0, respectively. RFJ is a Conselho Nacional de Desenvolvimento Científico e Tecnológico (CNPq) fellow under grant no. 304647/90-0.

References

[1] R.L. Peterson, J.W. Ekin, Phys. Rev. B 37 (1988) 9848.
[2] J.E. Evetts, B.A. Glowacki, Cryogenics 28 (1988) 641.
[3] E. Altshuler, J. Musa, J. Barroso, A.R.R. Papa, V. Venegas, Cryogenics 33 (1993) 308.
[4] K.H. Müller, D.N. Matthews, Physica C 206 (1993) 275.
[5] P. Muné, E. Altshuler, J. Musa, S. García, R. Riera, Physica C 226 (1994) 12.
[6] M. Mahel', J. Pivarc, Physica C 308 (1998) 147.
[7] L. Ji, M.S. Rzchowski, N. Anand, M. Tinkham, Phys. Rev. B 47 (1993) 470.
[8] M. Tinkham, J.C. Lobb, Solid State Phys. 42 (1989) 91.
[9] K.Y. Chen, Y.J. Qian, Physica C 159 (1989) 131.
[10] J.S. Xia, S.F. Sun, T. Zhang, L.Z. Cao, Q.R. Zhang, J. Chen, Z.Y. Chen, Physica C 158 (1989) 477.
[11] Y.J. Qian, Z.M. Tang, K.Y. Chen, B. Zhou, J.W. Qui, B.C. Miao, Y.M. Cai, Phys. Rev. B 39 (1989) 4701.
[12] M.J.R. Sandim, R.F. Jardim, Physica C 328 (1999) 246.
[13] F.C. Fonseca, R. Muccillo, Physica C 267 (1996) 87.
[14] E. Altshuler, S. García, J. Barroso, Physica C 177 (1991) 61.

[15] C.P. Bean, Rev. Mod. Phys. 30 (1964) 31.
[16] L. Mui, Supercond. Sci. Technol. 5 (1992) 208.
[17] E. Altshuler, R. Cobas, A.J. Batista-Leyva, C. Noda, L.E. Flores, C. Martínez, M.T.D. Orlando, Phys. Rev. B 60 (1999) 6373.
[18] Y.B. Kim, C.F. Kim, A.R. Strand, Phys. Rev. Lett. 9 (1962) 306.
[19] R.P. Barber Jr., R.C. Dynes, Phys. Rev. B 48 (1993) 10618.
[20] R. Haslinger, R. Joynt, Phys. Rev. B 61 (2000) 4206.